Available online at www.sciencedirect.com

ScienceDirect

Ceramics International 40 (2014) 1399–1404

CERAMICS INTERNATIONAL

www.elsevier.com/locate/ceramint

SPS sintering of silicon nitride with fluoride additive

Zafer Tatlı[a,*], Fatih Çalışkan[a], James Butler[b], Clare Crowley[b], Stuart Hampshire[b]

[a]Department of Metallurgical and Materials Engineering, Faculty of Technology, Sakarya University, 54187, Sakarya, Turkey
[b]Materials and Surface Science Institute, University of Limerick, Limerick, Ireland

Received 21 June 2013; received in revised form 21 June 2013; accepted 3 July 2013
Available online 20 July 2013

Abstract

Silicon nitride, one of the major structural ceramics, is sintered using additives such as Al_2O_3+MgO to provide conditions for liquid phase sintering to full density. The final microstructure contains high aspect ratio β-Si_3N_4 grains and intergranular glass. In this study, Spark Plasma Sintering (SPS) of silicon nitride, using Al_2O_3+MgO or MgF_2 as sintering additives, has been investigated in the temperature range 1400–1600 °C for 3 min since MgF_2 should produce liquid phases with lower melting temperatures than with MgO and therefore should sinter at lower temperature. Densification, microstructural development and mechanical behaviour have been compared. Maximum density (3.146 g cm^{-3}) was obtained for Si_3N_4+3% Al_2O_3+9.3% MgF_2 sintered by SPS at 1550 °C. In all samples, α- to β-Si_3N_4 transformation was incomplete but samples with MgF_2 showed higher β:α ratio than with MgO. Fluoride doped samples also exhibited higher fracture toughness than equivalent samples sintered with MgO.

Keywords: C. Mechanical properties; Silicon nitride; Fluoride additive; Spark plasma sintering; Densification

1. Introduction

Silicon nitride (Si_3N_4) has been developed over many years as a structural ceramic material which has superior toughness to many other ceramics, excellent strength at both room and elevated temperatures, good resistance to corrosive environments and excellent wear resistance, and is widely used in various engineering fields [1,2]. However, the relatively higher cost of ceramic parts compared to their metallic counterparts is a significant disadvantage that has limited its wider acceptance. Hence, an important direction for development of Si_3N_4 ceramics is to lower its production costs while maintaining its performance advantages [3].

Silicon nitride has highly covalent bonding and a low diffusivity of the constituents of the ceramic [1,4,5]. Because of this, sintering additives are required to obtain fully dense Si_3N_4 by various sintering techniques such as hot-pressing (HPSN), hot-isostatic pressing (HIPSN), Gas Pressure Sintering (GPS) and pressureless sintering. Densification proceeds via a liquid-phase sintering mechanism [1,2,5]. The liquid phase forms at high temperatures (1750–1900 °C) as a result of the reaction between the oxide sintering aids and the silica at the surface of the starting α-Si_3N_4 powder particles. This predominantly α silicon nitride phase is observed to transform to the β modification during the sintering process at temperatures in excess of 1400 °C. The α-Si_3N_4 dissolves in the M–Si–Al–O–N (M=Mg, Y, etc.) oxynitride liquid phase and is subsequently precipitated as β-Si_3N_4 which grows in the longitudinal direction as prismatic hexagonal rod-like crystals that eventually impinge on each other forming an interlocked microstructure. The liquid remains as a glass at the grain boundaries of the sintered materials after cooling, forming triple point junctions and nanoscale intergranular films (IGFs) [4,6,7]. The thickness of the IGF is very sensitive to the type of additive used and its concentration. The film thickness (in the range 0.5–1.5 nm) depends strongly on overall additive chemical composition [8,9].

It is well known that the amounts and ratios of the additives initially introduced determine the quantity and chemistry of the glass phase and this affects mechanical properties such as fracture toughness and flexural strength [1,2,7,10]. Substitution of nitrogen for oxygen in aluminosilicate glasses induces greater coordination of the glass network due to the tri-coordinate bonding of nitrogen compared to bi-coordinate bonding of oxygen, and this

*Corresponding author. Tel.: +90 2642956497; fax: +90 2642956424.
E-mail addresses: ztatli@sakarya.edu.tr, ztatli@gmail.com (Z. Tatlı).

0272-8842/$ - see front matter © 2013 Elsevier Ltd and Techna Group S.r.l. All rights reserved.
http://dx.doi.org/10.1016/j.ceramint.2013.07.021

results in increases in elastic modulus, hardness, glass transition temperature and viscosity of the glasses [11–13]. The effects of fluorine and nitrogen substitution for oxygen in calcium aluminosilicate glasses have been investigated [14–16]. It is a well known that fluorine as a non-bridging anion in oxide glasses acts as a powerful network disrupter [17].

The effect of fluorine addition on the structure of silicate or aluminosilicate glasses has been investigated [17–19] and it has been shown that fluorine can bond to silicon as Si–F and also to Al as Al–F [20,21]. In glasses containing both F and N, the network terminating effect of fluorine induces significant reductions in both glass melting temperatures (Tm) and glass transition temperatures (Tg) whilst elastic modulus and microhardness increase with nitrogen substitution for oxygen but are virtually unaffected by incorporation of fluorine [14,16].

Therefore, the question arises, if glass melting temperatures can be reduced by addition of fluorine but the beneficial effects of nitrogen on glass properties can be retained, would it be possible to use fluoride sintering additives for silicon nitride in order to reduce sintering temperatures whilst maintaining similar grain boundary glass characteristics? With this aim, some initial results on pressureless sintering of silicon nitride [22] and β-SiAlON [23] using fluoride additives showed that, following sintering at lower temperatures than normally used for silicon nitride (1550–1600 °C), fluoride additives gave higher densities and better mechanical properties than their oxide counterparts.

However, pressureless sintering requires longer sintering times at these lower temperatures compared with pressure-assisted sintering techniques to obtain fully dense materials. Over last few years, a new sintering method has been developed, Spark Plasma Sintering (SPS) [24,25], which allows densification of ceramics over fairly short time scales. This technique, also known as the field assisted sintering technique (FAST), uses an electrical current (DC, pulsed DC, or AC) which is passed through a conducting pressure die (graphite) and, if the material has reasonable electrical conductivity, through the ceramic itself. The die therefore acts as a heat source, so the sample is heated both internally and externally. The technique allows very rapid heating and cooling rates, very short holding times and results in densification at much lower sintering temperatures, usually a few hundred degrees lower than for conventional sintering. Spark Plasma Sintering of silicon nitride has resulted in fully dense materials with finer microstructures and much improved mechanical properties after much shorter sintering times at lower temperatures than conventional techniques [24,26–28].

In the present work, Al_2O_3+MgO or MgF_2 has been used as sintering additives in silicon nitride ceramics in order to produce liquid phases with lower melting temperatures. Comparisons have been made of densification and $\alpha \rightarrow \beta$ transformation during the Spark Plasma Sintering (SPS) process using either MgO or MgF_2 as additives with Al_2O_3.

2. Experimental

High purity starting powders were used as follows: α-Si_3N_4 (99.9% UBE, Industries, JAPAN), MgO (BDH Chemicals), Al_2O_3 (ALCOA) A17, and MgF_2 (Sigma Aldrich). The compositions of the various batches are shown in Table 1. These compositions were chosen in order to give the same Mg:Al:Si ratio in the final grain boundary glass composition. Mixed powders were ball milled with silicon nitride milling balls, using isopropyl alcohol as milling media for 24 h to ensure homogeneous mixing. The balls were subsequently removed and the slurry was firstly dried in a rotary evaporator and then dried at 100 °C in a standard oven for 4 h. and subsequently sieved through a 300 mesh sieve screen.

Table 1
The prepared compositions for SPS (wt%).

S3	91% α-Si_3N_4+3% Al_2O_3+6% MgO
FS3	91% α-Si_3N_4+3% Al_2O_3+9.3% MgF_2

Spark Plasma Sintering was performed using a Dr. Sinter Lab™ Model: SPS-515S (Syntex Inc., Kanagawa, Japan). Graphite mould interiors (10 mm in diameter) were lined with graphite paper and then a thin layer of boron nitride was sprayed on the inside to avoid contamination of the silicon nitride sample by the graphite mould and paper. Approximately 0.3 g of the prepared silicon nitride powder mixture was placed into the mould which gives a pellet of approximately 4 mm in thickness after sintering. The pressure applied was 25 MPa at all temperatures. The pulse schedule was 15 s on:5 s off. The sintering temperatures chosen were 1400, 1450, 1500, 1550 and 1600 °C at a heating rate of 200 °C/min and a dwell time of 3 mins.

Following SPS, the graphite paper was removed from the surfaces of the spark plasma sintered samples before commencing analysis. Density of the samples was measured using an Archimedean displacement technique. Scanning electron microscopy (SEM, JEOL, JSM-6700F, Japan) analysis was carried out to examine densification and residual pore distribution. The phases in the sintered products were analysed by X-ray diffraction (Rigaku, XRD D/MAX/2200/PC, Japan) using Cu Kα radiation and identified using X'Pert HighScore Report programme. Microhardness and fracture toughness testing [29] were carried out on samples using a microhardness tester model WH-402MVD (Instron ITW Co.). A total of 10 indentations were made on the surface of each sample.

3. Results and discussion

3.1. Densification behaviour

Fig. 1 shows displacement as a function of temperature during Spark Plasma Sintering (SPS) for silicon nitride powders with addition of alumina plus either MgF_2 or MgO densified up to 1600 °C. Shrinkage commences for the composition containing MgF_2 at 1300 °C and for that containing MgO at 1350 °C.

Thus, it appears that 1300 °C corresponds to the formation of the Mg–Si–Al–O–N–F liquid phase whereas the Mg–Si–Al–O–N liquid is known to form at 1350 °C [30]. Above these temperatures, densification continues at different rates and the

sample containing fluoride reaches a plateau at 1350 °C with a displacement of 2.4 μm whereas the sample containing MgO had only reached a displacement of 0.4 μm. This shows that the fluoride containing sample densified much faster than that containing only oxide additive.

The results of the densification of the spark plasma sintered samples are presented in Table 2 and Fig. 2. The highest density of 3.146 g cm^{-3} was obtained for Si_3N_4 with 3% Al_2O_3+9.3% MgF_2 (equivalent to 6% MgO) sintered at 1550 °C. The lowest density of 2.12 g cm^{-3} was recorded for Si_3N_4 with 3% Al_2O_3+6% MgO sintered at 1400 °C.

Whilst the maximum density was achieved at 1550 °C, densification decreased slightly at 1600 °C for both compositions and this can be explained by weight losses which are due to the volatility of magnesium-containing species at these temperatures. In general, samples containing fluoride have higher density values than the equivalent oxide containing samples. Thus, magnesium fluoride addition with alumina to silicon nitride can be considered as a beneficial sintering additive in the SPS process.

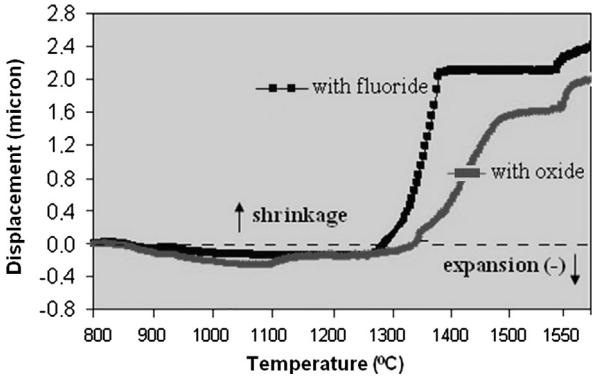

Fig. 1. Displacement as a function of sintering temperature for different additives for 3 min.

Table 2
Densities of silicon nitride with Al_2O_3+MgO (S3) or MgF_2 (FS3) spark plasma sintered at different temperatures for 3 min.

Temp. (°C)	Density (g cm^{-3})	
	S3	FS3
1400	2.12	2.70
1450	2.78	3.11
1500	3.05	3.14
1550	3.11	3.15
1600	3.09	3.14

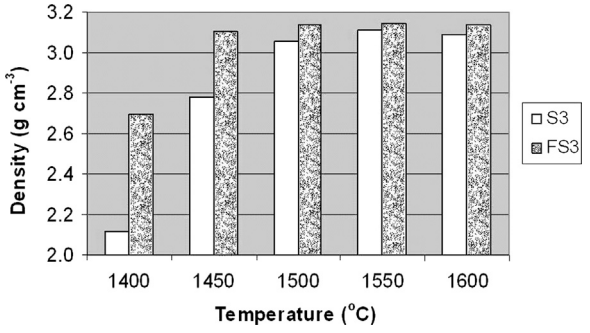

Fig. 2. Density of silicon nitride with Al_2O_3+MgO (S3) or MgF_2 (FS3) as a function of Spark Plasma Sintering temperature.

3.2. Microstructural analysis

Fig. 3 presents SEM micrographs of Si_3N_4 materials containing 3% Al_2O_3 and (a) 6% MgO and (b) 9.3% MgF_2 spark plasma sintered (SPS) at 1500 °C. Due to incomplete densification, a number of pores are present in the sample sintered using MgO. However, few pores are observed in the sample sintered with fluoride additive due to nearly complete densification. These microstructures are consistent with density results and displacement curves and show the effect of fluoride addition on liquid phase formation and densification.

3.3. XRD analysis of sintered samples

Fig. 4 shows the XRD pattern for Si_3N_4+3% Al_2O_3+6% MgO and Fig. 5 shows that for Si_3N_4+3% Al_2O_3+9.3% MgF_2, both spark plasma sintered at 1550 °C. The two strongest characteristic peaks for both α- and β-Si_3N_4 are

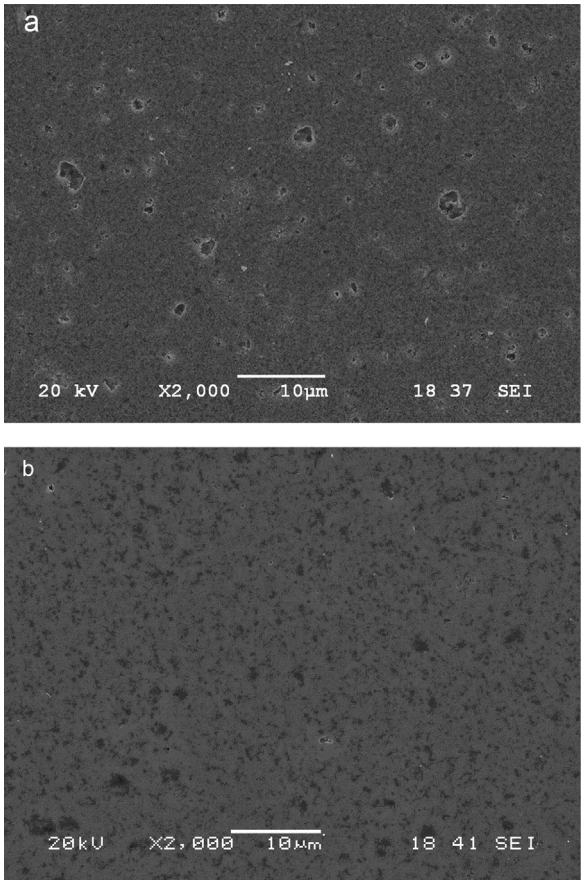

Fig. 3. SEM images of polished surfaces of silicon nitride sintered by SPS at 1550 °C for 3 min with 3% Al_2O_3 and (a) 6% MgO and (b) 9.3% MgF_2.

circled and these characteristic peaks were used to determine β:α+β phase ratio in all the samples. Table 3 shows the extent of α→β transformation for the two types of sintering additives at different temperatures. Transformation only commences for both additives at 1450 °C as expected from previous reports on silicon nitride [2,30]. In general, as temperature increases, the extent of α→β transformation increases and fluoride doped samples exhibit higher β:α ratios than those for MgO-doped samples although the amount of β formed is still quite limited as the dwell time at sintering temperature is very short (3 min). Although the dwell time is short for SPS compared with conventional sintering, the extent of α→β transformation is equivalent (after 3 min), to that achieved by pressureless sintering after 30 min [23]. Also, as with pressureless sintering, fluoride doped samples exhibit higher β/α ratios than the equivalent oxide dopant at 1550–1600 °C.

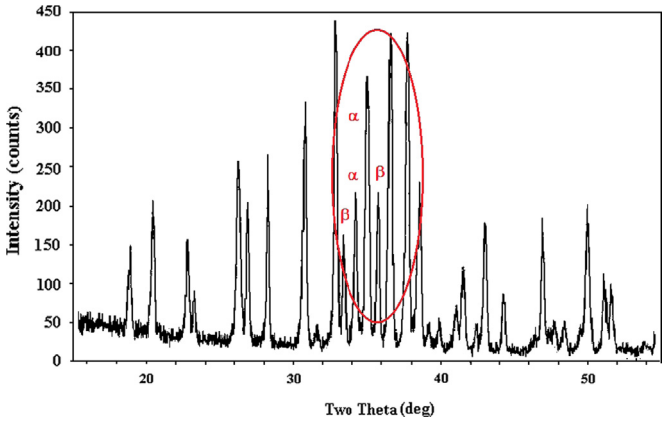

Fig. 4. X-ray diffraction pattern of silicon nitride with Al_2O_3+MgO sintered by SPS for 3 min at 1550 °C.

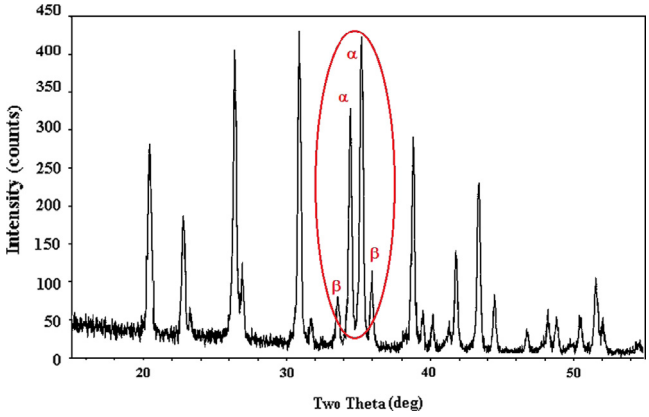

Fig. 5. X-ray diffraction pattern of silicon nitride with Al_2O_3+MgF_2 sintered by SPS for 3 min at 1550 °C.

Table 3
α→β transformation in samples sintered at different temperatures for 3 min by SPS.

Temp. (°C)	β/α+β ratio	
	S3	FS3
1400	nt	nt
1450	5	7
1500	5	12
1550	10	34
1600	26	40

nt: no α→β transformation.

The transformation occurs by dissolution of the α-phase Si_3N_4 into the liquid phase formed by the reaction of the additives with surface silica present on the Si_3N_4 grains. The more stable form of silicon nitride, β-Si_3N_4, is subsequently precipitated from the liquid and grows as elongated hexagonal grains. The dwell time during sintering would allow only a limited time for the transformation to proceed. Conventional methods have a much slower heating rate and the dwell times are considerably longer, thus allowing more time for the α→β transformation to proceed to completion.

Due to the fact that the fluoride-doped silicon nitride samples form liquid phases at a lower temperature and the fluorine-containing liquids allow higher solubility of nitrogen [14,15] than oxide samples, the liquid formed using MgF_2 allows greater solubility of nitrogen and also has more time to complete the α→β transformation compared to the samples containing MgO. The differences become more marked as temperature increases.

3.4. Mechanical properties of the spark plasma sintered silicon nitride

The mechanical properties of the SPS sintered samples with and without fluoride additives are given in Table 4. It can be seen that increases in both microhardness and fracture toughness are observed as the sintering temperature is raised, reflecting the increased density with increasing temperature. The highest value for microhardness of 1727 MPa for sample FS3 was achieved at a sintering temperature of 1550 °C, whereas for sample S3 the highest microhardness was 1839 MPa at 1600 °C. The highest values of fracture toughness were achieved at 1600 °C: 6.6 MPa $m^{1/2}$ for FS3 and 5.3 MPa $m^{1/2}$ for S3.

In general, FS3 Si_3N_4 samples containing MgF_2 have slightly lower microhardness compared with the S3 samples containing MgO whereas the fluoride containing samples have higher fracture toughness values than those for S3 at all temperatures. These differences in hardness and fracture toughness are due to the higher β:α ratio in FS3 (fluoride-containing) silicon nitrides compared with S3. It is well known that α-Si_3N_4 has higher hardness than β-Si_3N_4 owing to the stacking sequences of atoms in the crystal lattice whereas β-Si_3N_4 has higher fracture toughness than α due to the growth of elongated high aspect ratio rod-like β crystals which leads to self toughening for Si_3N_4 ceramics. Mechanical properties of fluorine-doped Si_3N_4-based ceramics and composites, using polytetrafluoroethylene (Teflon) as the source of fluorine, have been reported [31,32]. Segregation of fluorine was observed by TEM at grain and phase boundaries, leading to a decrease in the cohesive interfacial bond strength which then results in higher values for fracture toughness.

Table 4
MicroVickers hardness and fracture toughness of Si_3N_4 with Al_2O_3+MgO (S3) or MgF_2 (FS3) spark plasma sintered at various temperatures for 3 min.

Temp. (°C)	S3			FS3		
	Hardness HV1 (MPa) ±25		Kic (MPa $m^{1/2}$) ±0.1	Hardness HV1 (MPa) ±25		Kic (MPa $m^{1/2}$) ±0.1
1400	970	2 kg	–	960	2 kg	–
1450	1240		4.2	1160		4.5
1500	1395		4.8	1350		4.9
1550	1790		5.3	1727		5.5
1600	1839		5.3	1628		6.6

4. Conclusions

The densification of silicon nitride by Spark Plasma Sintering with alumina and MgO or MgF_2 sintering additives at temperatures from 1400 to 1600 °C for 3 min dwell time produced samples with between 67% and >99% theoretical density. The density of the samples increased with increasing sintering temperature. Fluoride addition results in formation of the sintering liquid phase at a lower temperature than for addition of MgO and thus densification commences at a lower temperature, thus allowing a greater degree of sintering of silicon nitride at all sintering temperatures. X-ray diffraction has shown that full transformation from α-Si_3N_4 to β-Si_3N_4 did not occur, the highest β/α+β ratio achieved being just 40% for the fluoride-containing sample and 26% for the oxide-doped sample at 1600 °C. Transformation during SPS is limited because of the high heating rate and short sintering time (3 min) but the use of fluoride allows greater solubility of the silicon nitride in addition to earlier formation of the sintering liquid.

The MgO-doped silicon nitrides had higher values of microhardness due to the higher α phase content whereas the MgF_2-doped samples exhibited higher fracture toughness which may be explained by the higher content of elongated β-phase crystals.

To summarise, the use of MgF_2 sintering additive in place of MgO during Spark Plasma Sintering of silicon nitride allowed better densification, higher α to β transformation and superior fracture toughness. This combination appears promising in terms of allowing sintering for very short times at relatively low temperatures.

References

[1] F.L. Riley, Silicon nitride and related materials, Journal of the American Ceramic Society 83 (2000) 245–265.
[2] S. Hampshire, Silicon nitride ceramics, Materials Science Forum 606 (2009) 27–41.
[3] L. Bai, X. Mao, W. Shen, C. Ge, Comparative study of β-Si_3N_4 powders prepared by SHS sintered by spark plasma sintering and hot pressing, Journal of University of Science and Technology 14 (2007) 271–275.
[4] S. Hampshire, The role of additives in the pressureless sintering of nitrogen ceramics for engine applications, Metals Forum 7 (1984) 162–170.
[5] G. Ziegler, J. Heinrich, G. Wötting, Relationships between processing microstructure and properties of dense and reaction-bonded silicon nitride, Journal of Materials Science 22 (1987) 3041–3086.
[6] H.J. Kleebe, M.K. Cinibulk, R.M. Cannon, M. Rühle, Statistical analysis of the intergranular film thickness in silicon nitride ceramics, Journal of the American Ceramic Society 76 (1993) 1969–1977.
[7] P.F. Becher, N. Shibata, G.S. Painter, F. Averill, K. Van Benthem, H.T. Lin, S.B. Waters, Observations on the influence of secondary Me oxide additives (Me=Si, Al, Mg) on the microstructural evolution and mechanical behavior of silicon nitride ceramics containing RE_2O_3 (RE=La, Gd, Lu), Journal of the American Ceramic Society 93 (2010) 570–580.
[8] D.R. Clarke, On the equilibrium thickness of ıntergranular glass phases in ceramic materials, Journal of the American Ceramic Society 70 (1987) 15–22.
[9] C.M. Wang, W.Q. Pan, M.J. Hoffmann, R.M. Cannon, M. Rühle, Grain boundary films in rare earth glass based silicon nitride, Journal of the American Ceramic Society 79 (1996) 788–792.
[10] E.Y. Sun, P.F. Becher, K.P. Plucknett, C.H. Hsueh, K.B. Alexander, S. B. Waters, et al., Microstructural design of silicon nitride with improved fracture toughness: II—effects of yttria and alumina additives, Journal of the American Ceramic Society 81 (1998) 2831–2840.
[11] S. Hampshire, R.A.L. Drew, K.H. Jack, Oxynitride glasses, Physics and Chemistry of Glasses 26 (1985) 182–186.
[12] S. Hampshire, Oxynitride glasses, Journal of the European Ceramic Society 28 (2008) 1475–1483.
[13] M.J. Pomeroy, S. Hampshire, SiAlON glasses, Journal of the Ceramic Society of Japan 116 (2008) 755–761.
[14] A.R. Hanifi, A. Genson, M.J. Pomeroy, S. Hampshire, Oxyfluoronitride glasses with high elastic modulus and low glass transition temperatures, Journal of the American Ceramic Society 92 (2009) 1141–1144.
[15] A.R. Hanifi, M.J. Pomeroy, S. Hampshire, Novel glass formation in the Ca–Si–Al–O–N–F system, Journal of the American Ceramic Society 94 (2011) 455–461.
[16] A.R. Hanifi, A. Genson, M.J. Pomeroy, S. Hampshire, Independent but additive effects of fluorine and nitrogen substitution on properties of a calcium aluminosilicate glass, Journal of the American Ceramic Society 95 (2012) 600–606.
[17] R. Hill, D. Wood, M. Thomas, Trimethylsilylation analysis of the silicate structure of flouro-alumino-silicate glasses and the structural role of fluorine, Journal of Materials Science 34 (1999) 1767–1774.
[18] E.M. Rabinovitch, On the structural role of fluorine in silicate glasses, Physics and Chemistry of Glasses 26 (1993) 157–165.
[19] J.F. Stebbins, Q. Zeng, Cation ordering at fluoride sites in silicate glasses: a high resolution F NMR study, Journal of Non-Crystalline Solids 262 (2000) 1–5.
[20] S.C. Kohn, R. Dupree, M.G. Mortuza, C.M.B. Henderson, NMR evidence for five and six coordinated aluminum fluoride complexes in F-bearing aluminosilicate glasses, American Mineralogist 76 (1991) 309–312.
[21] A. Stamboulis, R.V. Law, R.G. Hill, Structural characterization of fluorine containing glasses by F, Al, Si and P MAS-NMR spectroscopy, Journal of Non-Crystalline Solids 351 (2005) 3289–3295.
[22] F. Çalışkan, Z. Tatlı, S. Hampshire, H. Sönmez, V. Demir, Fabrication of silicon nitride with MgO/MgF_2 using pressureless sintering, in: M.M. Bucko, K. Haberko, Z. Pedzich, L. Zych (Eds.), Proceedings of the 11th ECERS Conference, European Ceramic Society, 2010, pp. 132–137.
[23] F. Çalışkan, Z. Tatlı, A. Genson, S. Hampshire, Pressureless sintering of β-SiAlON ceramic compositions using fluorine and oxide additive system, Journal of the European Ceramic Society 32 (2012) 1337–1342.

[24] M. Nygren, Z. Shen, On the preparation of bio-, nano- and structural ceramics and composites by spark plasma sintering, Solid State Sciences 5 (2003) 125–131.
[25] Z.A. Munir, U.T. Tamburini, M. Ohyanagi, The effect of electric field and pressure on the synthesis and consolidation of materials: a review of the spark plasma sintering method, Journal of Materials Science 41 (2006) 763–777.
[26] T. Nishimura, M. Mitomo, H. Hirotsuru, M. Kawahara, Fabrication of silicon nitride nano-ceramics by spark plasma sintering, Journal of Materials Science Letters 14 (1995) 1046–1047.
[27] H. Peng, Spark Plasma Sintering of Si_3N_4-Based Ceramics, Ph.D. thesis, Department of Inorganic Chemistry, Stockholm University, Sweden, 2004.
[28] M. Suganuma, Y. Kitagawa, Pulsed electric current sintering of silicon nitride, Journal of the American Ceramic Society 86 (2003) 387–394.
[29] A.G. Evans, E.A. Charles, Fracture toughness determinations by indentation, Journal of the American Ceramic Society 59 (1976) 371–372.
[30] S. Hampshire, K.H. Jack, The kinetics of densification and phase transformation in nitrogen ceramics, Proceedings of **British Ceramic Society** 131 (1981) 37–49.
[31] H.J. Kleebe, G. Pezzotti, T. Nishida, Transmission electron microscopy characterization of fluorine-doped Si_3N_4, Journal of Materials Science Letters 14 (1995) 1668–1671.
[32] H.J. Kleebe, G. Pezzotti, T. Nishida, M. Rühle, Role of interface structure on mechanical properties of fluorine-doped Si_3N_4–SiC ceramics, Journal of the Ceramic Society of Japan 106 (1998) 17–24.